THE OFFICIAL MAGAZINE OF THE OCEANOGRAPHY SOCIETY

Oceanography

CITATION

St. Laurent, L., H. Simmons, T.Y. Tang, and Y.H. Wang. 2011. Turbulent properties of internal waves in the South China Sea. *Oceanography* 24(4):78–87, http://dx.doi.org/10.5670/oceanog.2011.96.

DOI

http://dx.doi.org/10.5670/oceanog.2011.96

Turbulent Properties of Internal Waves in the South China Sea

BY LOUIS ST. LAURENT, HARPER SIMMONS, TSWEN YUNG TANG, AND YUHUAI WANG

ABSTRACT. Luzon Strait and South China Sea waters are among the most energetic internal wave environments in the global ocean. Strong tides and stratification in Luzon Strait give rise to internal waves that propagate west into the South China Sea. The energy carried by the waves is dissipated via turbulent processes. Here, we present and contrast the relatively few direct observations of turbulent dissipation in South China Sea internal waves. Frictional processes active in the bottom boundary layer dissipate some of the energy along China's continental shelf. It appears that more energy is lost in Taiwanese waters of the Dongsha Plateau, where the waves reach their maximum amplitudes, and where the bottom topography abruptly shoals from 3,000 m in the deep basin to 1,000 m and shallower on the plateau. There, energy dissipation by turbulence reaches 1 W m^{-2}, on par with the conversion rates of Luzon Strait.

R/V *Ocean Researcher* 3 off Dongsha Reef during August 2008. Waves breaking on the reef are visible in the distance. The photo was taken from R/V *Ocean Researcher 1*, which was nearby. *Photo courtesy of Victor Cappella*

INTRODUCTION

The regional waters around Taiwan consist of the Philippine Sea to the East, Luzon Strait to the south, and the South China Sea to the west. Strong monsoons and the world's most active tropical cyclone season characterize this area. The Kuroshio current dominates the circulation east of Taiwan, meandering up through Luzon Strait where the complex topography of Lan-Yu and Heng-Chun Ridges steer the flow. Strong mixed diurnal and semidiurnal barotropic tides characterize the ridge system (Beardsley et al., 2004). The combination of tides, topography, and stratification of the Kuroshio frontal zone results in some of the strongest internal wave generation in the global ocean (Simmons et al., 2011, in this issue). Internal waves, in the forms of internal tides and nonlinear wave packets, radiate into the South China Sea and deposit their energy as turbulence along the basin margins.

Turbulence, in the form of breaking internal waves, is the primary mechanism for mixing the ocean interior's thermodynamic properties. Of primary concern is the mixing of heat, which, together with salinity, produces buoyancy flux to modify stratification. The mixing of heat is also important to the biology of the upper ocean, where animals such as corals are sensitive to cycles of warming and cooling. Turbulent mixing also acts on the nutrient properties of the upper ocean, further influencing biological activity. Turbulent processes driven by internal waves radiated from Luzon Strait significantly influence Dongsha Atoll, 370 km

southwest of Taiwan in the South China Sea (Wang et al., 2007).

Much attention has been focused on nonlinear internal wave packets that develop as the internal tide evolves over time and moves downstream, toward the continental margin of China (Farmer et al., 2009). The Asian Seas International Acoustics Experiment (ASIAEX) was the first large-scale study of these phenomena. Several papers describe time-series measurements of the waves (Duda et al., 2004; Ramp et al., 2004; Yang et al., 2004). Orr and Mignerey (2003) recorded shoaling waves using high-frequency acoustic imagery, revealing details of wave evolution along the continental slope. Their images show the conversion of depression waves into elevation waves near the 200 m isobath. Specific wave packets were tracked by ship, and simultaneous acoustic Doppler current profiler (ADCP) velocity measurements were used to estimate wave energy. Orr and Mignerey (2003) reported significant energy exchange between individual crests as the wave groups spread over larger horizontal length scales. They also observed instabilities in the form of wave overturns. Although turbulence levels were not measured directly, ADCP-derived estimates of kinetic energy suggest large amounts of wave energy are lost through turbulence during the conversion process as the waves shoal.

Additional work during ASIAEX included moored ADCP measurements (Lien et al., 2005; Chang et al., 2006). These data were interpreted as showing a strong divergence of kinetic energy as

the Luzon Strait waves shoal, presumably due to dissipation by friction and turbulence. Lien et al. (2005) find that the shelf-break region of the northern South China Sea typically exhibits four times the baroclinic energy of the typical mid-latitude open ocean. Based on these studies, it is reasonable to expect that the South China Sea has one of the most dissipative margins in the global ocean.

Here, we present direct measurements of turbulent dissipation levels made during the period 2005 to 2010. These measurements are the first attempt to characterize the turbulence properties across the South China Sea region where the internal waves that originate in Luzon Strait decay. We present observations of oceanic microstructure, where shear is measured on centimeter to millimeter scales. At such scales, the shear variance of the turbulent dissipation subrange is resolved, and estimates of the turbulent kinetic energy dissipation rate can be made. Estimates of dissipation are done over $O(1)$ m vertical bins based on spectral analysis of the microshear signal (e.g., Lueck et al., 2002). Diffusivities, as formulated from the dissipation rate under the assumption that the turbulent kinetic energy budget is in statistical steady state for large ensembles, are calculated using a mixing efficiency of 20%, according to Osborn (1980). Together, the dissipation rate and the diffusivity characterize the level of mixing influencing the stratification. In all cases described here, microstructure measurements were made using free-falling, tethered, vertical profiling instruments. In most

cases, we used a Rockland Scientific VMP-500 or VMP-2000 Vertical Microstructure Profiler, described on the Rockland Scientific website (http://rocklandscientific.com).

Our assessment considers turbulence measurements taken across the South China Sea starting with measurements collected in the continental shelf region studied during ASIAEX. We will then discuss measurements along the Dongsha Plateau, and conclude with some preliminary turbulence measurements in Luzon Strait.

THE CONTINENTAL SHELF REGION WEST OF TAIWAN

Taiwan Strait is the very shallow passage between mainland China and the island of Taiwan. Shallow-water processes dominate the turbulence in such a region, most likely in the form of a full-depth bottom boundary layer driven by strong tides and local wind-driven currents. A sinuous continental slope region lies just south of Taiwan Strait, where the waves generated in Luzon Strait shoal from depths exceeding 3,000 m to depths as shallow as 40 m. The shoaling process is extremely violent, and the transformation of depression waves (waves that propagate along near-surface stratification) to trains of elevation waves (waves that propagate along a near-bottom density interface) was well documented during ASIAEX (Orr and Mignerey, 2003; Duda et al., 2004). Local internal wave generation, via the interaction of tides with the shelf and continental slope, also contributes to the wave activity.

Gawarkiewicz et al. (2004) point out that the depth structure of the buoyancy field during April and May along the
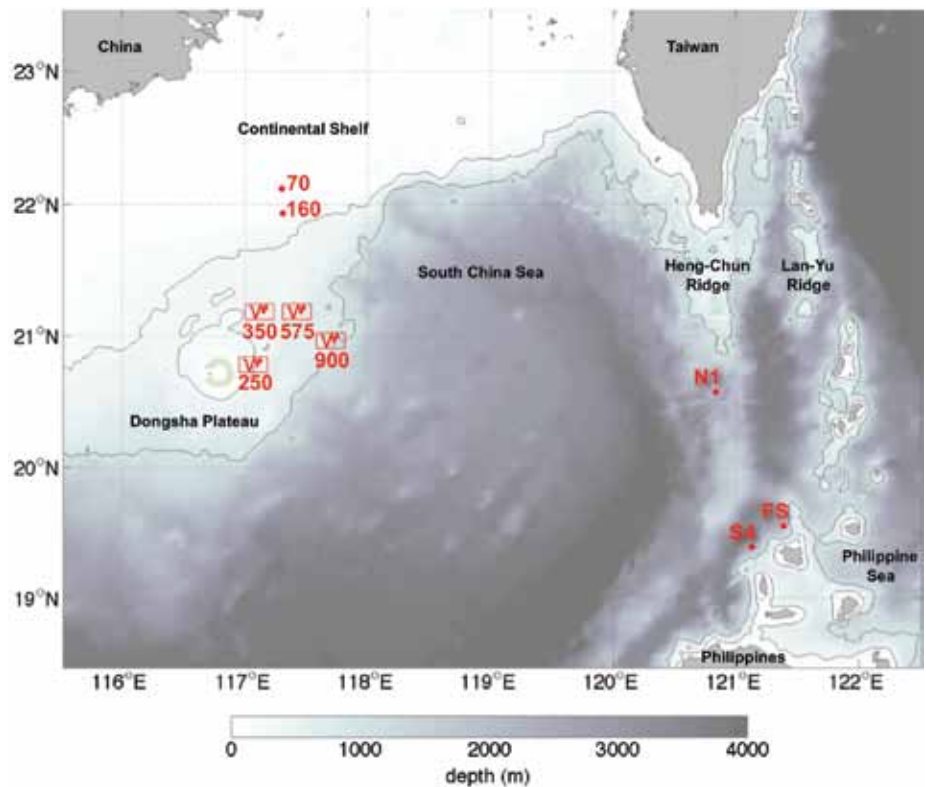

Figure 1. Map showing the South China Sea region around Taiwan. Gray shading shows the bathymetry. The 300 m and 1,000 m isobaths are also shown by contours. Red symbols indicate the locations where direct measurements of turbulence have been made. The wave icons indicate cases of specific wave-packet turbulence observations, with numerical values indicating the depth of the site in meters.

northern South China Sea shelf break depends on the state of the transition between the winter and summer monsoon. During ASIAEX in April and May of 2001, the winter monsoon ended in March, and the shelf break stratification structure was rather shallow, with a buoyancy gradient maximum at 20 m depth. During seasons when the winter monsoon lingers into April, the buoyancy gradient maximum stays between 50 and 100 m depth, preventing the formation of elevation waves.

During April 2005, a 10-day field survey was conducted on the continental slope and shelf of the South China Sea on the Taiwanese vessel *Ocean Researcher 1* (*OR1*). R/V *OR1*

is a 60 m regional class survey vessel operated by National Taiwan University. Turbulence measurements, described by St. Laurent (2008), were made along a section spanning the shelf-break region, as indicated by the 70 m and 160 m isobaths in Figure 1. The section spans the primary worksite of the ASIAEX study. A composite section of dissipation across the shelf region showed column-integrated dissipation levels exceeding 50 mW m^{-2} between the 100 m and 200 m isobaths, in contrast to 10 mW m^{-2} levels seaward and shoreward of this region. The overall average is 25 mW m^{-2}, an order of magnitude larger than the average open-ocean dissipation rate for tidal energy (Munk and

Wunsch, 1998). Taken with estimates of the buoyancy frequency, diffusivity estimates given by Osborn (1980) along the shelf-break region exceed 1 cm^2 s^{-1}, also an order of magnitude above open-ocean values.

Time-series data collected at the 160 m (Figure 2a) and 70 m (Figure 2b) isobaths show examples of high-frequency internal wave activity and associated turbulence levels along the shelf. These 10-hour time series, recorded on April 15 and 17, 2005, respectively, show wave activity via the fluctuation of temperature isotherms as measured by the turbulence profiler. Turbulent dissipation levels reach 1 x 10^{-5} W kg^{-1} in the upper and lower

boundary layers, and also in the stratified interior where wave shear produces instability. Depth-integrated values of dissipated power range from 10 to 100 mW m^{-1}, about half of which can be accounted for by frictional processes acting in the bottom boundary layer.

St. Laurent (2008) describes baroclinic energy flux estimates for the shelf break, based on data from the 160 m isobath.

This limited record shows maximum energy flux of 8 kW m^{-1}, and a mean of 3.8 kW m^{-1}. The latter is very close to the Chang et al. (2006) estimate for this region's internal tide energy flux, based on their much longer current meter record. Chang et al. (2006) estimate that nonlinear waves comprise 20% of the baroclinic energy flux at the shelf break, a much-diminished fraction relative

Louis St. Laurent (lstlaurent@whoi.edu) is Associate Scientist, Department of Physical Oceanography, Woods Hole Oceanographic Institution, Woods Hole, MA, USA. Harper Simmons is Associate Professor, School of Fisheries and Ocean Sciences, University of Alaska Fairbanks, Fairbanks, AK, USA. Tswen Yung Tang is Professor, Institute of Oceanography, National Taiwan University, Taipei, Taiwan. YuHuai Wang is Associate Professor, Institute of Applied Marine Physics and Undersea Technology, National Sun Yat-sen University, Kaohsiung, Taiwan.
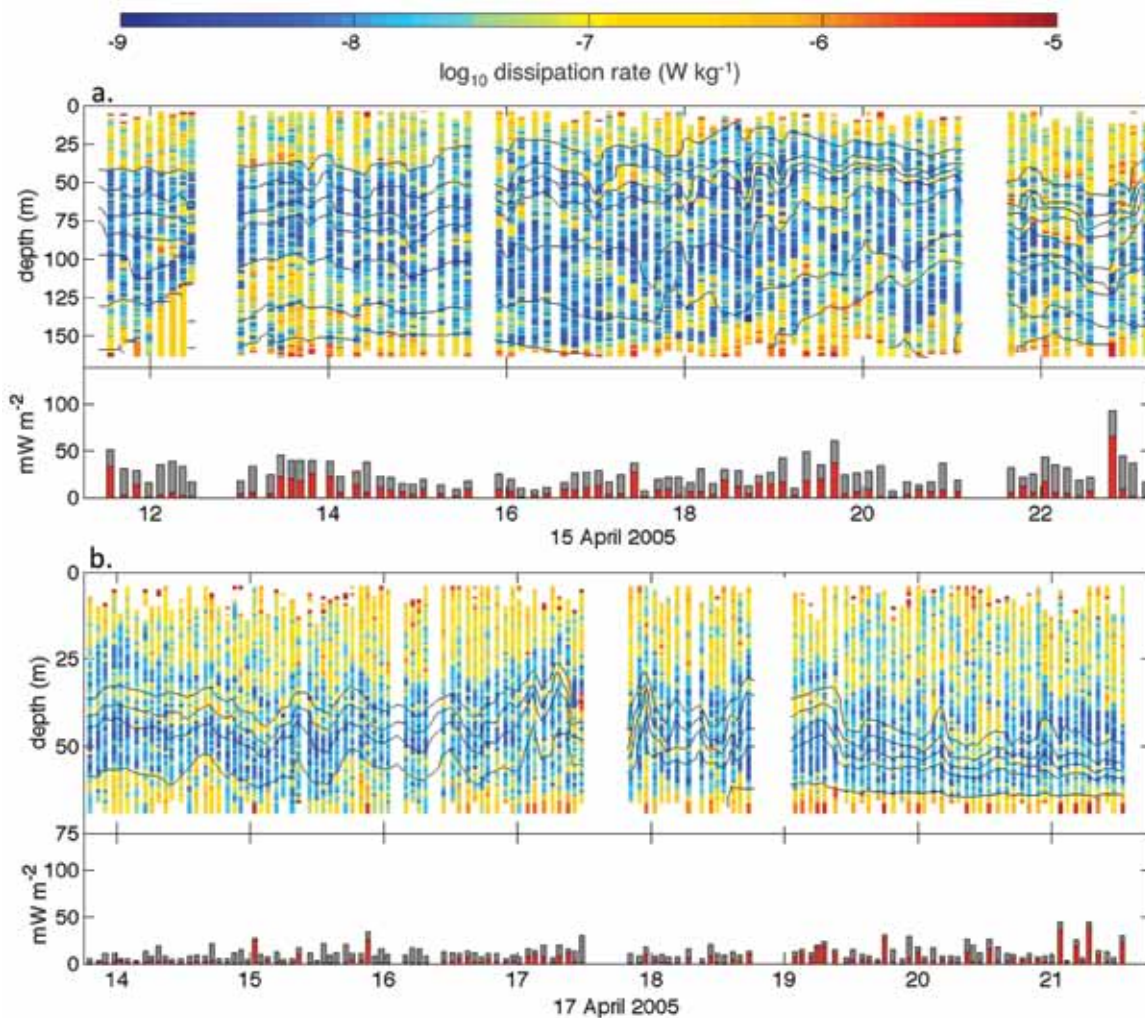
Figure 2. Observations of internal wave activity and turbulence at the 160 m (a) and 70 m (b) isobaths on the continental shelf region west of Taiwan. Temperature contours indicate the fluctuations of layers associated with high-frequency internal waves. Turbulent dissipation rates are shown according to a logarithmic color axis, as indicated by the color bar. Depth-integrated values of density times dissipation rate are shown along the bottom panels. Red bars indicate the level of dissipation accounted for by bottom friction.

to the nearby Dongsha Plateau. Our results support the finding of Chang et al. (2006) that much of the baroclinic energy of the Luzon waves is dissipated before reaching the continental shelf off China. This result makes the observed dissipation levels all the more impressive, as the trickle of Luzon energy that propagates onto the South China Sea shelf break still drives one of the most dissipative coastal regions of the ocean. The more direct path of Luzon-generated internal waves is discussed in the following section.

THE DONGSHA PLATEAU

A unique aspect of the South China Sea is the Dongsha Plateau, a broad region of the continental slope extending nearly halfway across the basin. The plateau ranges in depth from 1,500 m to less than 300 m before merging with the continental shelf. Dongsha Atoll sits distinctly along the plateau and is 25 km across.

The primary beam of internal wave energy generated in Luzon Strait points directly toward Dongsha Plateau, and waves very abruptly shoal from 3,000 m to 1,500 m. Most dramatically, soliton-like depression waves hit the plateau on their westward path across the basin. Given the enormous energy levels associated with these anomalies, strong turbulence levels would seem to be a likely property of the wave-shoaling process. However, despite some detailed observational studies of these waves (Klymack et al., 2006; Alford et al., 2011), direct measurements of their turbulence levels were taken only during the present co-authors' recent surveys using Taiwan research vessels. Here, we present observations from two such surveys.

During the period April 28 to May 4, 2007, the Taiwanese research vessel *Ocean Researcher 3* (*OR3*) surveyed the region around Dongsha Reef for internal wave activity (Figure 1). R/V *OR3* is a 40 m coastal class survey vessel operated

by National Sun Yat-sen University. The survey activity was interrupted on numerous occasions by foul weather, during which R/V *OR3* would seek refuge in the lee (west) of Dongsha Atoll. Survey activities were thus intermittent to the atoll's east. However, a coherent soliton-like internal wave was spotted on the ship's radar along the 1,500 m isobath at 21.09°N, 117.98°E. The timing corresponded to the period of maximum spring tides. We believe the subsequent turbulence measurements represent the first time dissipation rates were directly measured in a South China Sea solitary wave, and the first time ever that direct dissipation measurements were recorded in any wave of comparable scale and amplitude.

Figure 3 shows turbulence profiles made in rapid succession through the wave pulse during the period 0030 to 0220 UTC on May 4. Backscatter, as measured from the EK500 120 kHz system, is shown in color. In what
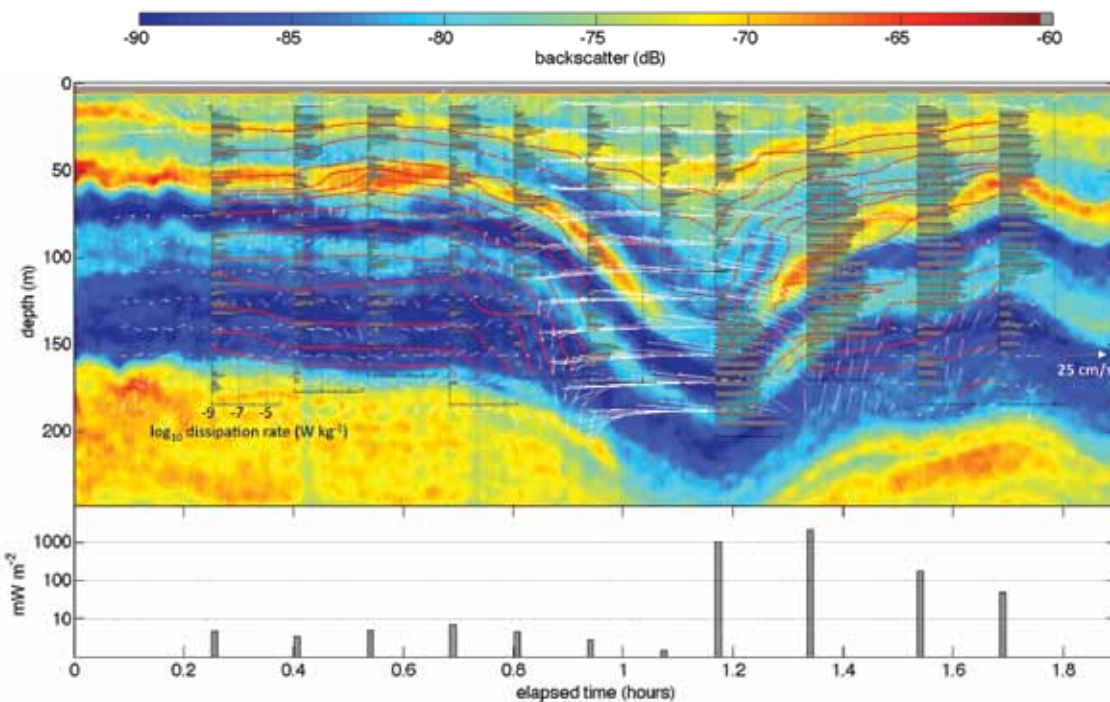

Figure 3. An observation of an internal wave pulse at the 900 m isobath near 21°N, 117.5°E, in the South China Sea, observed on May 4, 2007. Acoustic backscatter (120 kHz) reveals the general structure of the wave. Acoustic Doppler current profiler-measured velocity vectors, profiler-measured temperature (red contours), and turbulent dissipation rates are also shown (reference axis on left-most profile). The wave speed is 2.5 m s^{-1}. Depth-integrated values of density times dissipation rate are shown along the bottom panel.

appears to be the core of the wave, the temperature field shows significantly perturbed structure. Behind the core, overturns in the temperature structure are also clearly present (corresponding to overturns in density). ADCP-measured velocity vectors show a dynamically rich pattern of currents occurring through the wave pattern. Vertical velocities exceed 0.25 m s^{-1} in the wake of the wave core, and their counterclockwise rotation is consistent with a westward-propagating wave, with downward advection of isotherms ahead of the core, and upward advection of isotherms behind the core.

Figure 3 also provides estimates of turbulent dissipation. There is significant contrast between the dissipation levels in the leading half of the wave and those in the wave's wake. Levels slightly greater than 1 x 10^{-9} W kg^{-1} characterize wave arrival, dramatically increasing to values O(10^2) to O(10^5) times larger in the wave core and wake. The peak values occur at the trailing edge of the apparent core, with dissipation values of 1 x 10^{-4} W kg^{-1} characterizing density overturns exceeding 30 m in vertical extent. This level of turbulent dissipation is comparable to another recent observation in a South China Sea wave core (Lien et al., in press). The lower panel of Figure 3 shows integrated levels of dissipated power, computed by depth-integrating the dissipation rate times the density. Integrated dissipation levels rise from O(10) mW m^{-2} in the leading half of the wave to O(1) W m^{-2} in the wake of the wave. The wake values are extraordinary by oceanographic standards, as the global mean level of dissipation required for closing the tidal energy budget is only 3 mW m^{-2} (Munk

and Wunsch, 1998).

There are two major implications here. First, the buoyancy flux associated with the wave core's mixing is rather limited, as the fluid is already well mixed, preventing the strong turbulence from accessing much buoyancy gradient to act on. While there is clearly buoyancy flux in the wake, where overturns in temperature (and density) are visible (Figure 3), the effective diffusivity is not straightforward to calculate in the case of active overturning. If the background buoyancy gradient were applicable to the turbulence levels in the core of the wave, the turbulent diffusivity would reach 0.1 m^2 s^{-1} for a mixing efficiency of 20%. This figure is 10,000 times the open-ocean thermocline value of 1 x 10^{-5} m^2 s^{-1} (St. Laurent and Simmons, 2006). This estimate, while providing a useful reference, is not necessarily meaningful given the uncertainties about mixing efficiency in extremely well-mixed stratifications (St. Laurent et al., 2001). A more sensible mean estimate of diffusivity can be done for the tail of the wave, as Figure 4 shows. For this estimate, data from the last two profiles of Figure 3, where the density profile was stable, were used to estimate the diffusivity. We find values in the range from 1 x 10^{-4} m^2 s^{-1} to 1 x 10^{-3} m^2 s^{-1}.

The large-amplitude

depression waves that traverse the Dongsha Plateau exhibit a dramatic transformation as they shoal. In the above example, at the 900 m isobath, the wave maintained a soliton-like form typical of waves observed in the deeper basin (Klymak et al., 2006), despite the large turbulence levels characterizing the core of the wave. In shallower water, the waves eventually split into trains of waves (e.g., Orr and Mignerey, 2003; Duda et al., 2004). During this process, it is reasonable to assume that energy dissipation is significant.

Some direct turbulence measurements of this process were collected on the Dongsha Plateau along 21°N near 117°E in August 2008 during a survey on R/V *OR1* (Figure 5). The region is just northeast of Dongsha Atoll, and the area
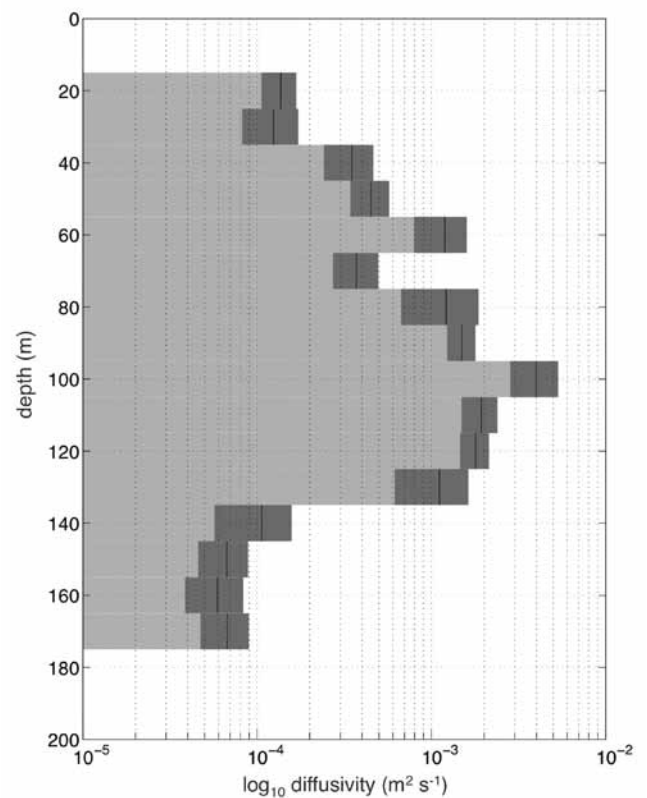

Figure 4. Diffusivity estimate for the wake of the wave event shown in Figure 3. Confidence intervals (95%) are shown by the shaded bands about each bin's mean.

has been a primary focus during internal wave studies. During the 2008 survey, a depression anomaly was tracked as it passed from the 575 m to 375 m isobaths over a period of 5.5 hours. As it shoaled, what was originally a single depression pulse split into a pair (Figure 5). Using the leading depression pulse as a marker, an average speed of 1.9 m s⁻¹ applies to the packet over the 24 km distance between the two observations.

During the transition from one to two pulses, turbulence levels increase in the tail, or wake, of the wave packet. Integrated dissipation levels increase by a factor of two during this transition, reaching maximum levels of 50 mW m⁻² in the profile between the two depression anomalies in the later event. Most of the increase occurs below 100 m depth, in the primary stratified layer, where the displacement between the density surfaces is largest.

The exact nature of mechanisms acting to elongate the train of depressions in this shoaling process remains unclear, though nonlinear dispersion is clearly at play. Much attention has been paid to the conversion of depression waves into elevation waves, for example, along the New Jersey shelf of the US Mid-Atlantic Bight (Shroyer et al., 2010). Such conversion occurs along the Dongsha Plateau as well, at points further to the west than our presented observations.

LUZON STRAIT

In contrast to the turbulence levels observed in the wave dissipation region of the South China Sea, turbulence levels in the internal wave-generation region of Luzon Strait are not directly attributable to nonlinear waves. Instead, turbulence levels seem to be associated with the energetic cycle of tidal forcing in the passage. Model estimates (Simmons et al., 2011, in this issue) suggest that the largest baroclinic generation sites in Luzon Strait exceed 10 W m⁻², which is consistent with the magnitude of observed internal wave fluxes into the South China Sea.

During August 14–September 12, 2010, a field survey was conducted on the US research vessel *Roger Revelle*. Alford et al. (2011) report on the mooring and lowered ADCP survey results from that cruise. Here, we report on measurements of upper-ocean
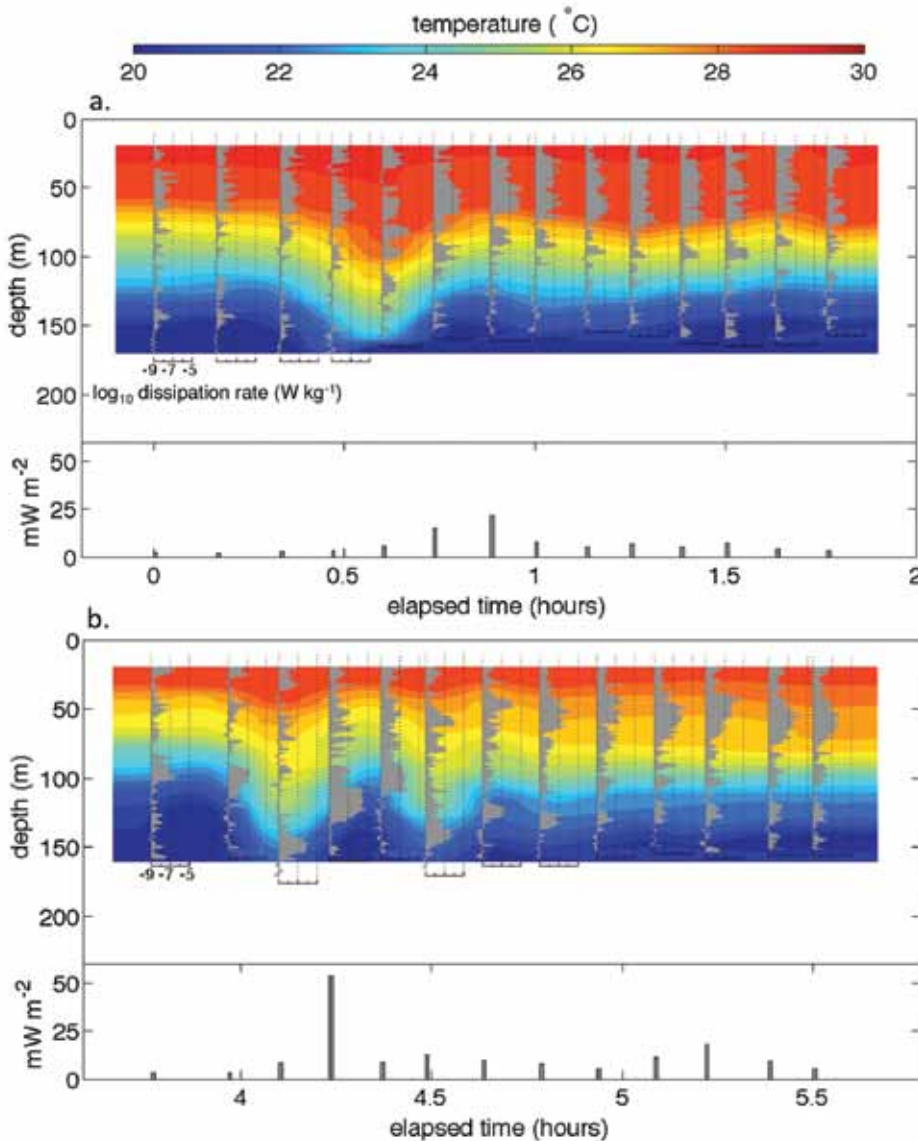

Figure 5. Time series showing the evolution of the Dongsha Plateau depression anomaly. The initial wave pulse exhibited a single depression anomaly shoaling along the 575 m isobath northeast of Dongsha Atoll (a). After two hours of measurements conducted by sailing the vessel along the wave front, we ran ahead of the wave to the 375 m isobath 24 km west of the original observation site. There, the wave had evolved into a two-pulse depression anomaly (b). Turbulent dissipation rate profiles are shown for each case, and integrated levels of dissipated power are shown in the lower panel of each time series. Temperature contours, indicating the stratification, are shown according to the color bar.
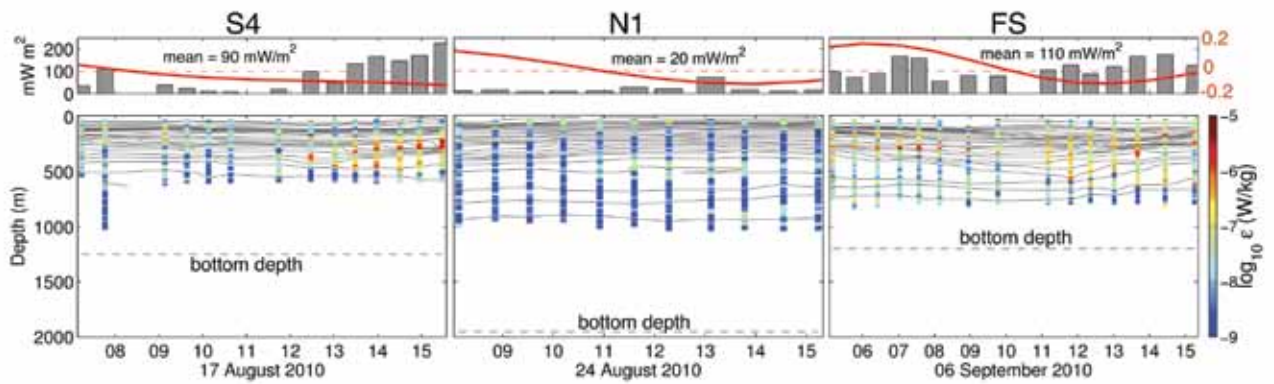
Figure 6. Time-series observations of upper-ocean turbulence measured at stations S4, N1, and FS (Figure 1) near the ridges in Luzon Strait. The x-axis is time in hours UTC, with the year, month, and day indicated. The lower panels show isotherms on one-degree intervals overlain by dissipation. The upper panels show depth-integrated dissipation (gray bars) and east-west tidal velocity from the TOPEX/Poseidon global tidal model (TPXO) in meters per second (right axis, red lines) in central Luzon Strait (a proxy for the local tide because phase is nearly uniform over the ridge complex). Dashed gray lines in each lower panel indicate local bottom depth.

dissipation from three time-series stations (Figure 6). Stations S4, N1, and FS (Figure 1) were occupied for eight, seven, and ten hours, respectively.

Dissipation was enhanced at S4 and FS but relatively weak at N1, with station mean values of 90, 110, and 20 mW m^{-2}, respectively. These estimates reflect the integrated dissipation over the upper 600 m, and thus underestimate the total dissipation at each site, as bottom depths range from 1,200 to 2,000 m (as indicated in Figure 6). It appears that dissipation was enhanced at the end of the occupation of stations S4 and N1 and at the beginning and end of station FS. These periods of larger dissipation coincide with tidal extrema (ebb or flood tides), although it is difficult to draw a definitive conclusion. The dissipation occurs at mid-depth, away from surface or bottom boundary layers. Although sites of large wave generation are not exactly coincident with the S4, N1, and FS measurement sites, the model-mean conversion rate over an area bounded by 20°N to 21°N and 121.5°E to 122°E is 750 mW m^{-2}. These three stations do not

represent dissipation rates that are a large fraction of the total wave generation, and would suggest that much of the baroclinic energy input radiates away from the ridges to be dissipated elsewhere.

CONCLUSION

Figure 7 is a schematic representation of the phenomena described in our study. In the internal wave generation region of Luzon Strait, nonlinear wave anomalies have not been observed. Instead, turbulence levels are supported by strong shear, presumed to be associated with processes such as internal wave beams (Simmons et al., 2011, in this issue). West of Luzon Strait, the strong internal tide evolves into large-amplitude depression waves (Farmer et al., 2009), which propagate at speeds near 3 m s^{-1} (Klymak et al., 2006). The depression waves reach Dongsha Plateau, where they rapidly shoal and experience strong turbulent dissipation. As the depression anomalies shoal further, they elongate into trains, eventually becoming elevation waves as they propagate onto the continental shelf, continuing to dissipate energy

through turbulence.

The story of turbulent dissipation in Taiwan's South China Sea and Luzon Strait waters is still incomplete. The small number of observations made using direct profiling measurements of turbulence suggest that the largest turbulence levels occur in the fully developed wake of a large-amplitude depression anomaly on the Dongsha Plateau. There, depth-integrated dissipation levels reach 1 W m^{-2} over the upper 250 m.

We have explored dissipation data in other scenarios, including dissipating wave energy on the continental shelf, shoaling waves on the Dongsha slope, and turbulent events in Luzon Strait. In all of these cases, integrated dissipation levels were O(10) to O(100) mW m^{-2}, well below the levels observed in the large-amplitude wave on Dongsha Plateau. To our knowledge, no direct measurements of dissipation have been made in the largest of the South China Sea wave anomalies occurring in the deep water of the basin between Luzon Strait and the Dongsha Plateau.

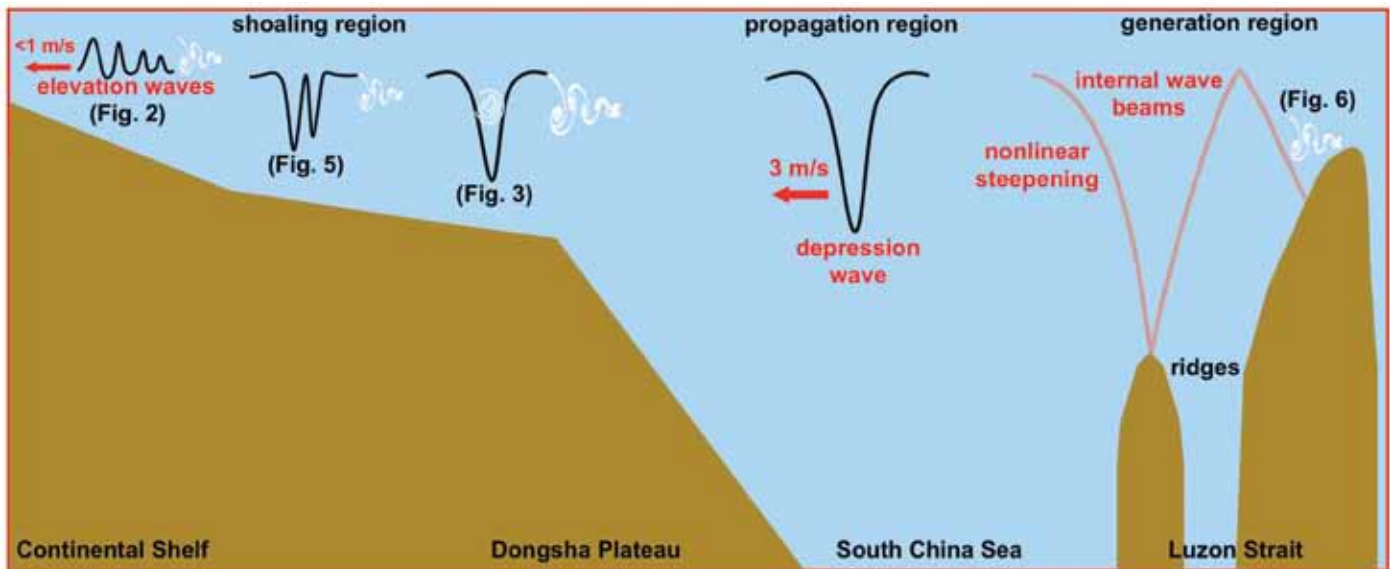The existing data lead us to speculate

Figure 7. Schematic representation of the internal wave and turbulence phenomena of the South China Sea. Turbulent processes are represented by eddies and vortices (in white). References to figures showing examples of the observed phenomena are indicated.

that most internal wave dissipation in the South China Sea occurs in the large-amplitude waves along the Dongsha Plateau, where the waves begin their shoaling process in the relatively deep slope region. This region is perhaps where the maximum balance exists between wave energy level and instability. Further to the east, the waves may have larger amplitudes, but they have not had time to develop enough shear to create turbulence. Further to the west, the waves are more uniformly turbulent from leading edge to tail, but the energy levels have diminished to lesser values.

A crude assessment of the energy flux divergence of waves crossing the South China Sea would suggest that roughly 10 kW m^{-1} is dissipated in the zone between 119°E and 117°E, where the wave energy flux diminishes from over 10 kW m^{-1} (Klymak et al., 2006) to roughly 1 kW m^{-1} (St. Laurent, 2008). This dissipation level would require an average depth-integrated dissipation rate of 50 mW m^{-2}. Thus, the dissipation

levels observed in the wave along the 900 m isobath are perhaps larger than needed on average, while the dissipation rates observed at the shallower sites are perhaps smaller than needed on average. So, perhaps the dissipation rates even out to the required level. Additional dissipation measurements would be helpful for careful assessment.

The South China Sea and Luzon Strait comprise a large area, and more general assessments of the turbulence characterizing the background internal wave environment have been initiated using direct dissipation measurements (Tian et al., 2009) and indirect inferences based on finestructure of the velocity and density field (Alford et al., 2011). Forthcoming Luzon Strait measurements are anticipated as part of the joint Taiwan and US Internal Waves in Straits Experiment (IWISE) measurement program. An adequate assessment of South China Sea turbulence levels will require considerable additional work using both direct and indirect methods.

REFERENCES

Alford, M.H., J.A. MacKinnon, J.D. Nash, H.L. Simmons, A. Pickering, J.M. Klymak, R. Pinkel, O. Sun, L. Rainville, R. Musgrave, and others. 2011. Energy flux and dissipation in Luzon Strait: Two tales of two ridges. *Journal of Physical Oceanography*, http://dx.doi.org/10.1175/JPO-D-11-073.1.

Beardsley, R.C., T.F. Duda, J.F. Lynch, J.D. Irish, S.R. Ramp, C.-S. Chiu, T.Y. Tang, Y.-J. Yang, and G. Fang. 2004. Barotropic tide in the northeast

South China Sea. *IEEE Journal of Oceanic Engineering* 29:1,075–1,086, http://dx.doi.org/10.1109/JOE.2004.833226.

Chang, M.-H., R.-C. Lien, T.Y. Tang, E.A. D'Asaro, and Y.J. Yang. 2006. Energy flux of nonlinear internal waves in northern South China Sea. *Geophysical Research Letters* 33, L03607, http://dx.doi.org/10.1029/2005GL025196.

Duda, T.F., J.F. Lynch, J.D. Irish, R.C. Beardsley, S.R. Ramp, C.-S. Chiu, T.Y. Tang, and Y.J. Yang. 2004. Internal tide and nonlinear internal wave behavior at the continental slope in the northern South China Sea. *IEEE Journal of Oceanic Engineering* 29:1,105–1,130, http://dx.doi.org/10.1109/JOE.2004.836998.

Farmer, D., L. Qiang, and J.-H. Park. 2009. Internal wave observations in the South China Sea: The role of rotation and non-linearity. *Atmosphere-Ocean* 47:267–280, http://dx.doi.org/10.3137/OC313.2009.

Gawarkiewicz, G., J. Wang, M. Caruso, S.R. Ramp, K. Brink, and F. Bahr. 2004. Shelfbreak circulation and thermohaline structure in the northern South China Sea: Contrasting spring conditions in 2000 and 2001. *IEEE Journal of Oceanic Engineering* 29:1,131–1,143, http://dx.doi.org/10.1109/JOE.2004.839123.

Klymak, J.M., R. Pinkel, C.-T. Liu, A.K. Liu, and L. David. 2006. Prototypical solitons in the South China Sea. *Geophysical Research Letters* 33, L11607, http://dx.doi.org/10.1029/2006GL025932.

Lien, R.-C., T.Y. Tang, M.H. Chang, and E.A. D'Asaro. 2005. Energy of nonlinear internal waves in the South China Sea. *Geophysical Research Letters* 32, L05615, http://dx.doi.org/10.1029/2004GL022012.

Lien, R.-C., E.A. D'Asaro, F. Henyey, M.H. Chang, T.Y. Tang, and Y.J. Yang. In press. Trapped core formation within a shoaling nonlinear internal wave. *Journal of Physical Oceanography*.

Lueck, R.G., F. Wolk, and H. Yamazaki. 2002. Oceanic velocity microstructure measurements in the 20th century. *Journal of Oceanography* 58:153–174.

Munk, W., and C. Wunsch. 1998. Abyssal recipes II: Energetics of tidal and wind mixing. *Deep-Sea Research Part I* 45:1,977–2,010, http://dx.doi.org/10.1016/S0967-0637(98)00070-3.

Orr, M.H., and P.C. Mignerey. 2003. Nonlinear internal waves in the South China Sea: Observation of the conversion of depression internal waves to elevation internal waves. *Journal of Geophysical Research* 108, 3064, http://dx.doi.org/10.1029/2001JC001163.

Osborn, T.R. 1980. Estimates of the local rate of vertical diffusion from dissipation measurements. *Journal of Physical Oceanography* 10:83–89, http://dx.doi.org/10.1175/1520-0485(1980)010<0083:EOTLRO>2.0.CO;2.

Ramp, S.R., D. Tang, T.F. Duda, J.F. Lynch, A.K. Liu, C.-S. Chiu, F. Bahr, H.-R. Kim, and Y.J. Yang. 2004. Internal solitons in the northeastern South China Sea: Part I. Sources and deep water propagation. *IEEE Journal of Oceanic Engineering* 29:1,157–1,181, http://dx.doi.org/10.1109/JOE.2004.840839.

Shroyer, E., J. Moum, and J. Nash. 2010. Energy transformations and dissipation of nonlinear internal waves over New Jersey's continental shelf. *Nonlinear Processes in Geophysics* 17:345–360, http://dx.doi.org/10.5194/npg-17-345-2010.

St. Laurent, L. 2008. Turbulent dissipation on the margins of the South China Sea. *Geophysical Research Letters* 35, L23615, http://dx.doi.org/10.1029/2008GL035520.

St. Laurent, L., and H. Simmons. 2006. Estimates of power consumed by mixing in the ocean interior. *Journal of Climate* 19:4,877–4,890.

St. Laurent, L., J.M. Toole, and R.W. Schmitt. 2001. Buoyancy forcing by turbulence above rough topography in the abyssal Brazil Basin. *Journal of Physical Oceanography* 31:3,476–3,495, http://dx.doi.org/10.1175/1520-0485(2001)031<3476:BFBTAR>2.0.CO;2.

Simmons, H., M.-H. Chang, Y.-T. Chang, S.-Y. Chao, O. Fringer, C.R. Jackson, D.-S. Ko. 2011. Modeling and prediction of internal waves in the South China Sea. *Oceanography* 24(4):88–99, http://dx.doi.org/10.5670/oceanog.2011.97.

Tian, J., Q. Yang, and W. Zhao. 2009. Enhanced diapycnal mixing in the South China Sea. *Journal of Physical Oceanography* 39:3,191–3,203, http://dx.doi.org/10.1175/2009JPO3899.1.

Wang, Y.H., C.F. Dai, and Y.Y. Chen. 2007. Physical and ecological processes of internal waves on an isolated reef ecosystem in the South China Sea. *Geophysical Research Letters* 34, L18609, http://dx.doi.org/10.1029/2007GL030658.

Yang, Y.J., T.Y. Tang, M.H. Chang, A.K. Liu, M.-K. Hsu, and S.R. Ramp. 2004. Solitons northeast of Tung-Sha Island during the ASIAEX pilot studies. *IEEE Journal of Oceanic Engineering* 29:1,182–1,199, http://dx.doi.org/10.1109/JOE.2004.841424.